Characterization of Mirror Birefringence for ALPS

Harrison LaBollita
University of Florida
hlabollita0219@lions.piedmont.edu
August 4, 2017

Abstract

Mirror birefringence has created new challenges for many experiments requiring mirrors. In this paper, I use a heterodyne polarimeter to characterize the linear birefringence of mirrors, specifically spatially and in a magnetic field. These measurements will be used to assist ALPS researchers to measure vacuum magnetic birefringence. It was found that a ThorLabs BB1-E03 dielectric mirror varies approximately 7% across the probed surface area of the mirror. For a New Focus 5104, a ThorLabs BB1-E03, and a mirror made with fused silica, the induced magnetic stress on the mirror caused no measurable difference in the linear birefringence of these mirrors.

Introduction

One of the most exciting developments in modern physics is looking for new particles outside the Standard Model, such as the axion and axion-like particles. Axion-like particles could be a constituent of dark matter, which accounts for over 80% of all the matter in the universe [5]. Discovery of these new particles in a certain parameter space could also explain unaccounted-for observations, such as, the increased transparency of the universe seen in the TeV spectra of gamma rays found from blazers. The Any Light Particle Search (ALPS) experiment targets exactly this parameter space.

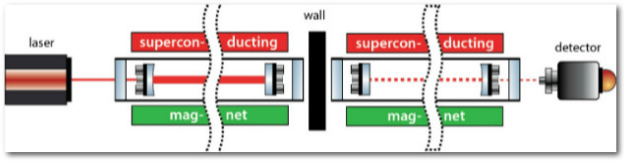

Figure 1.1 A general picture of the ALPS II experiment. The laser on the left will shine light into the production cavity surrounded by superconducting magnets producing millions of axion-like particles. The axion-like particles will pass through the wall entering the regeneration cavity on the right, in which, they will oscillate back into photons. These photons will be detected by a photodetector [5].

The ALPS experiment consists of ALPS I and ALPS II, which are both light shining through a wall experiments. ALPS I was the beginning of the ALPS experiment and it ran from 2007 until 2010. ALPS II will consist of two optical cavities approximately 100m in length surrounded with 5T superconducting magnets and a light-tight barrier in between them. *Figure 1.1* is a conceptual illustration of the ALPS II experiment. Laser light is shone into the production cavity, where the magnetic field induces the photons to convert into axion-like particles that traverse through the wall, then convert back into photons in the regeneration cavity. Thus, light will have been shown through a wall. ALPS II contains multiple phases ALPS IIa, IIb, and IIc. ALPS IIa began in 2015, and its purpose is to test a 10m optical cavity intended for the next iteration of ALPS. ALPS IIb was skipped and we are now in ALPS IIc. ALPS IIc is the final iteration of ALPS II. The general setup mentioned above is currently being finalized and is projected to begin recording data in 2019.

The general setup of ALPS also contains the equipment necessary to observe vacuum magnetic birefringence (VMB). Recall, birefringence is an optical property that causes a phase shift in light dependent upon their polarizations. The ALPS II optical cavities can be utilized as a vacuum chamber, which can be permeated with high magnetic field, and with additional optical components, this will be a sufficient environment to measure VMB. VMB claims that light traveling through a vacuum permeated with a magnetic field will experience a birefringent effect. VMB is one of the last predictions of QED that has yet to be seen experimentally [3,5]! Because VMB is an extremely subtle effect ($\Delta n_{vmb} \approx 10^{-22}$ for ALPS), the sensitivity of the experiment must be extremely high.

The ALPS experiment requires numerous optical components. Optics have a birefringent property that can result in unwanted effects. In our case, mirrors introduce new challenges. The birefringence of mirrors is undetermined and has not yet been quantified. This could manifest a problem, because the VMB signal might be dominated by the noise introduced by the birefringence in the mirrors. Therefore to measure VMB, the birefringence of mirrors must be known and characterized.

In this paper, I use an optimized heterodyne polarimeter to measure the intrinsic birefringence of several mirrors. I examine how the intrinsic birefringence changes spatially across the surface of the mirror and how the birefringence changes in the presence of a magnetic field. These measurements will assist ALPS researchers to ascertain the most effective way to eliminate the unwanted effects of the mirrors from the measurement so that VMB is successfully detected.

Birefringence

2.1 General Birefringence

Birefringence can be formally defined as the optical property of a material having a refractive index that depends upon the polarization and propagation direction of light [1]. It is quantified as

$$\Delta n = n_e - n_o$$

where Δn is the maximum difference between the refractive indices n_e (extraordinary light ray) and n_o (ordinary light ray). The refractive index of a medium is defined as

$$n = \frac{c}{v}$$

where c is the speed of light in a vacuum and v is the speed of light in the material.

Birefringence is most commonly seen in anisotropic crystals. Due to their anisotropy, these crystals have orientation dependent optical axes, known as the fast and slow axes. Light rays can be decomposed into two orthogonal polarization components; these components are then governed by their interaction with the crystal. When light enters an anisotropic crystal in the direction of the

optical axis, it behaves similarly to interaction with isotropic crystals and passes through with a single index of refraction [1]. However, when light enters the crystal off-axis, the two orthogonal components will experience different refractions. Thus when the two polarization components exit the anisotropic crystal the light ray will be phase shifted altering the total polarization of the light ray.

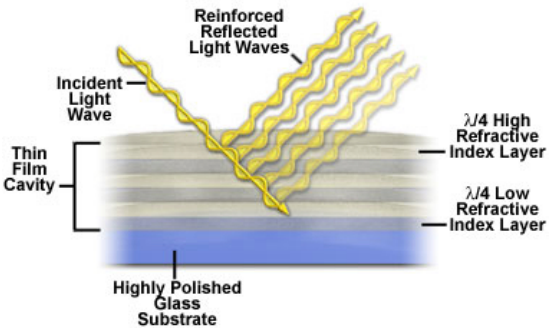

Figure 2.2.1 A diagram of a dielectric mirror is shown above. The dielectric material coatings are layered on top of a substrate in an alternating fashion. Partial reflections occur at each dielectric layer [*6*].

2.2 Mirror Birefringence

Highly reflective mirrors are constructed on top of a substrate that is then coated with dielectric materials having alternating high and low indices of refraction [2]. These layers have optical thicknesses $\lambda/4$, where λ is the wavelength of light for which the reflectivity of the layer is optimized [2]. *Figure 2.2.1* is an illustration of the construction of a dielectric mirror. A portion of the incident light wave is reflected after each interface with the dielectric layers, producing coherent light waves that constructively interfere [*6*]. This results in a highly reflective mirror.

Mirror birefringence can be attributed to a wide range of effects that have not been evaluated in detail. These effects include: deficiencies in the mirror coatings, an intrinsic material property of the coatings, and/or stress.

These mirror coatings create an optical cavity that light must travel through before being reflected. When light reflects off of the "surface" of the mirror, the beam must travel some optical distance through these reflective layers before finally being reflected and exiting the reflective layers. It is in this process where the birefringent effect takes place. This manifests a problem when conducting a measurement because the mirrors induce a phase difference, which then superimposes on the signal to be measured [*2*]. Inconsistencies in mirror coatings would lead to varying birefringent effects of the mirror. This makes it imperative to study mirror birefringence as these inconsistencies would lead to spatially dependent birefringence.

ALPS will be using 5T superconducting magnets that will permeate their optical cavities. The mirrors used in these cavities will be within the stray magnetic field of the superconducting magnets. In the presence of a magnetic field, these mirror coatings could be susceptible to physical alterations. Magnetic induced stress on the mirror coatings could change the birefringent effect of the mirror. Thus, it is imperative to understand how the birefringence of mirrors changes in the pres-

ence of the magnetic field.

Methods

3.1 Heterodyne Polarimeter

I used a heterodyne polarimeter to measure the linear birefringence of our mirrors. This device acted as a probe for which we could quantitatively measure the birefringence of mirrors. This was achieved by measuring the relative phase difference between two orthogonally polarized laser beams incident on a mirror, or in general, a birefringent source (BF source). *Figure 3.1.1* is a schematic of our heterodyne polarimeter, which consisted of two 1064 nm lasers, three photodetectors (PDs), a BF Source, and an assortment of other optics.

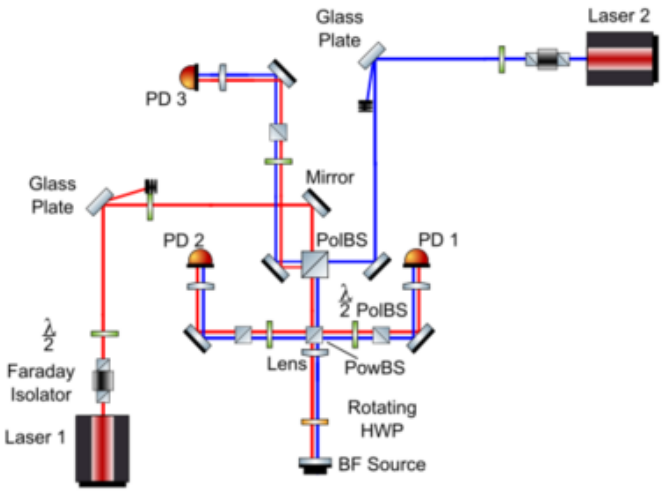

Figure 3.1.1 Above is a schematic of the heterodyne polarimeter used to measure the intrinsic birefringence. Two laser beams are orthogonally overlapped and then split, so that half of the beam is sent into a reference photodetector and the other half the beam is reflected off of birefringent source, which causes a relative phase difference and is then measured by a second photodetector.

The two lasers (L1 and L2) were overlapped in a heterodyne interferometric setup on a central polarizing beam splitter and locked at a beat frequency of 5MHz. Faraday isolators were mounted in front of the laser beams to prevent unwanted back reflections into the laser beams. To control the power going into the central polarizing beam splitter (PolBS), two half-wave plates (HWPs) were mounted after the Faraday isolators. By rotating the HWPs, we could control the amount of power that was transmitted through and reflected by the PolBS.

We positioned glass plates to reduce the beam power of L1 and L2 to make them more comparable once they were overlapped into the central PolBS. Mirrors were used to steer L1 and L2 into the first PolBS.

The first PolBS was used to isolate the p-polarization of the L1 beam and the s-polarization of the L2 beam, so that the beams were orthogonally polarized going into the power beam splitter (PowBS). The central PolBS was also used to send the two beams into our third photodetector PD3. The polarization of light from L1 that was not transmitted through the central PolBS was reflected and then steered through a mirror, another PolBS to isolate the horizontal component of the polarization then passed through a lens to focus the beam onto the diode of PD3. We isolated the horizontal component of the

beam, because the beat frequency is maximized when the two laser beams are overlapping and in the same polarization.

For L2, the polarization of light that was not reflected in the PolBS was transmitted through and then followed the same path to PD3. Our third photodetector was necessary for locking the beat frequency of L1 and L2.

The orthogonally polarized beam entered the 50:50 PowBS so that half of the beam was sent towards the optics leading to PD2 and the other half was sent towards the BF Source.

The beam traveling towards the PD2 went through a HWP to rotate the polarization of the beam, then through a PolBS to isolate the horizontal component of the polarization so that the both beams contributed about the same amount of power to the 5MHz beat note when entering the PD2. Finally, the beam is then reflected off a mirror and sent through a lens to focus onto the diode of PD2. PD2 was used as a reference signal to the signal entering PD1.

The light that was transmitted towards the BF Source first passed through a rotating HWP controlled by a brushless motor. The rotating HWP effectively rotated the orientation of the beam's orthogonal polarizations at four times the rotation frequency of the HWP. The beam then reflected off of the BF source acquiring a relative phase difference, travelled back through the rotating HWP (which stops the rotation) then back into the PowBS, after which the beam was reflected into another HWP to rotate the polarization, then through a PolBS to isolate the horizontal component of the polarization, and sent through a lens to focus the beam onto the diode of PD1. This is our birefringent signal.

The beat frequency entering PD1 had a relative phase difference to the beat frequency entering PD2. In our experiment, the rotating HWP had a rotation frequency of 5Hz, so the relative phase difference should appear at 20Hz, since this phase difference was oscillating at four times the rotation frequency.

3.2 Laser Locking

High precision lasers are ubiquitous in optical physics. They are an essential component to precision measurements in optics. Unfortunately, the short-term stability of these lasers are inadequate for many of their applications. This makes it necessary to implement a laser locking technique to lock the beat frequency of the lasers. This will allow the frequencies of the lasers to drift, but their beat frequency, the difference of the two lasers, will be stable. *Table 3.2.1* is a table of the laser locking electronics used in our experiment. A detailed report of the laser locking technique used in our experiment can be found in [*3*].

Table 3.2.1

Component	Frequency	Impedance
TDS 2024 Oscilloscope	200 MHz	1 MΩ
HP 8591E Spectrum Analyzer	9kHz-1.8GHz	50Ω
ThorLabs PDA10CF InGaAs Amplified Photodetector	1.5 GHz maximum	
SRS DS345 Synthesized Function Generator	30MHz	50Ω
Mini-Circuits BLP-5+ Low Pass Filter	DC-5MHz	50Ω
Mini-Circuits ZFRSC-42 S+ Splitter	DC-4200MHz	50Ω
Mini-Circuits ZAD-6+ Mixer	0.003-100MHz	
Mini-Circuits ZF3RSC-542-S+	DC-5400MHz	50Ω

Table 3.2.1 Above is a table of the electronics used in the laser locking scheme for the heterodyne polarimeter.

3.3 Data Collection and Analysis

Data from PD1 and PD2 was collected using a Moku:Lab phase meter instrument by Liquid Instruments [*4*], which can be seen in *Figure 3.3.1*. The Moku:Lab compared the phase of both of our beat notes with respect to a universal reference clock. The data was logged at a 120 S/s, saved to a CSV file, then processed in MATLAB.

The difference between PD1 and PD2 was taken so that any common mode noise between the two beat notes would be subtracted leaving only the phase shift do to our mirrors. This difference was used to calculate the Fast Fourier Transform (FFT) using MATLAB. The FFT would allow us to see our 20Hz birefringent signal from which we could then extrapolate the magnitude of our signal in units of μrad. This data would allow us to create contour plots in MATLAB that would give us a visual representation of how the birefringence was changing across the surface of the mirror. This would also allow us to see how the amplitude of the birefringent signal changed do to the influence of a magnetic field.

Figure 3.3.1 Above is an image of a Moku:Lab device that we used to collect all of our data. The interface of the Moku:Lab is controlled via iPad and the corresponding iPad application. The Moku:Lab and iPad are linked via a wireless network [*4*].

3.4 Magnetic Field

To induce magnetic stress on our mirrors, we purchased four N52-Neodymium magnets (BY0X06-N52) from K&J Magnetics, Inc., which we mounted in mounts that I designed specifically for our experiment.

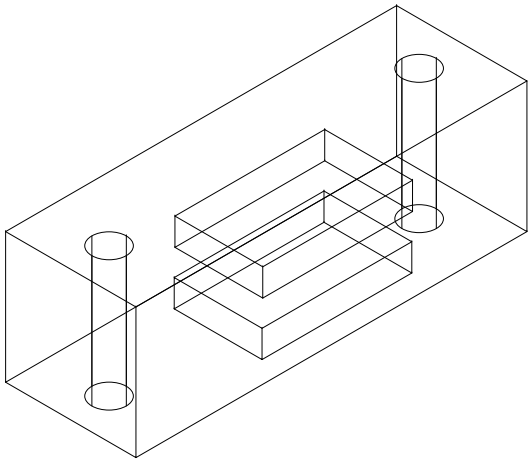

Figure 3.4.1 A schematic of the magnet mount drawn in AutoCAD 2015. The dimensions of the box are 5 1/8" x 1 7/8" x 1 3/8", with cavities for our magnets to be inserted as well as cavities for the poles the mount to be mounted to.

Figure 3.4.1 is a schematic of the mounts I designed for the experiment. *Figure 3.4.3* shows the magnet mounts in our experiment with the magnets installed. Each individual mount can house two bar magnets, and with two of these mounts we can house a total of four bar magnets.

The neodymium magnets we purchased were 2" x 1" x 3/8" and were advertised to have a surface field of 3411 gauss. We measured the magnetic field of one of these magnets (*see Figure 3.4.2)* and found the measured magnetic field to be very close to the theoretical magnetic field. We measured all of the magnetic fields with a F.W. Bell 6010 Gauss/Tesla Meter.

The following equation was used to calculate the theoretical magnetic field over distance for a permanent magnet,

$$B = \frac{B_r}{\pi} arctan\left(\frac{LW}{2z\sqrt{4z^2 + L^2 + W^2}}\right) - arctan\left(\frac{LW}{2(D+z)^2\sqrt{4(D+z)^2 + L^2 + W^2}}\right)$$

where B_r is the remanence field, z is the distance away from a pole of the magnet, L is the length of the magnet, W is the width of the magnet, and D is the thickness of the magnet. Units are arbitrary as long as they are all consistent.

The magnetic field needed to be parallel to the surface of the mirror, otherwise we would be seeing a Faraday effect from our magnets, not magnetic stress induced birefringence. Our mounts were designed in order to maximize the parallel magnetic field at the surface of the mirror so that we could see the largest affect possible.

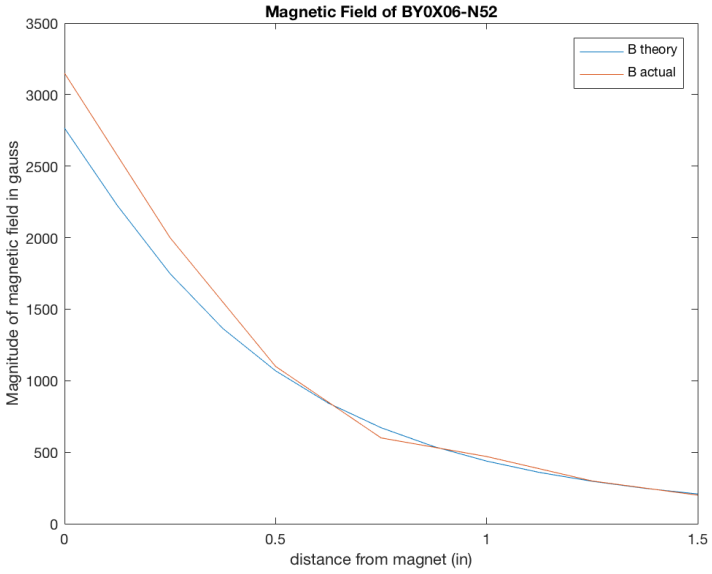

Figure 3.4.2 Plots of the magnetic field with respect to distance. The blue curve is the theoretical magnetic field and the red curve is the measured magnetic field.

We calculated the expected magnetic field and measured the actual magnetic field for two and four magnets (see *Figure 3.4.4)*. This gave us a good approximation for the field we expect the surface of the mirror to experience. This is not the identical magnetic field ALPS will experience, but in general, this will give us insight into how the birefringence of a mirror is affected in the presence of a magnetic field.

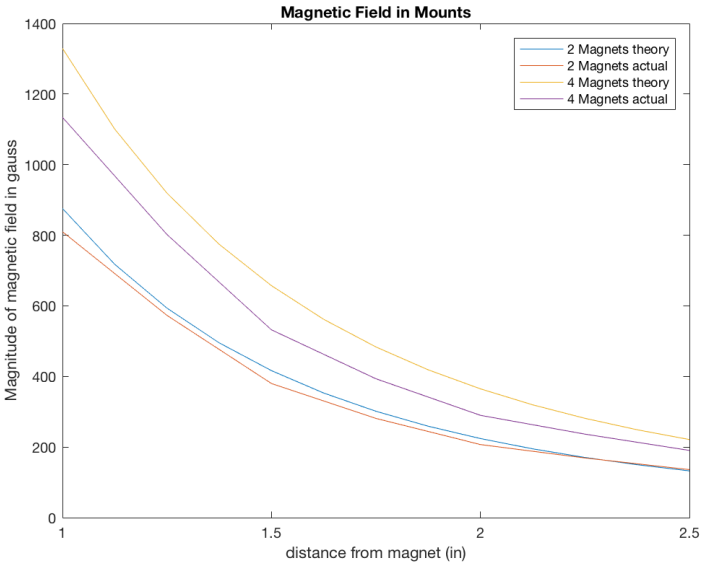

Figure 3.4.4 Plots of magnetic field with respect to distance. The blue curve is the theorized curve with two magnets. The red is the measured curve with two magnets. The yellow is the expected curve with four magnets. The purple is the measured curve.

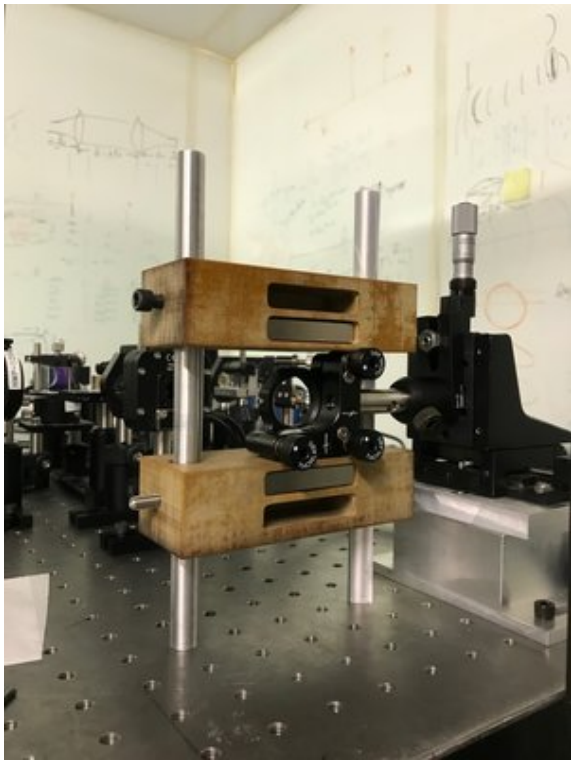

Figure 3.4.3 The mounts installed in our experiment. These mounts were made out of a non-magnetic material called phenolic.

Results and Discussion

4.1 Spatial Variations

Measurements were taken at discrete points on the surface of the mirror in a grid-like manner. The mirror was mounted in a ThorLabs 6XS mirror mount and suspended in a Newport 460-XYZ mount. The mirror's surface was repositioned to coincide with a 4x4 grid centered about the center of the mirror. The 4x4 grid consisted of 16 total points with each point being 4mm apart from one another. This allowed us to effectively examine an area of 144 mm^2. The beam size for which we were probing the surface of the mirror was approximately 1mm. *Figures 4.1.1-2* show a mapping of the surface of the

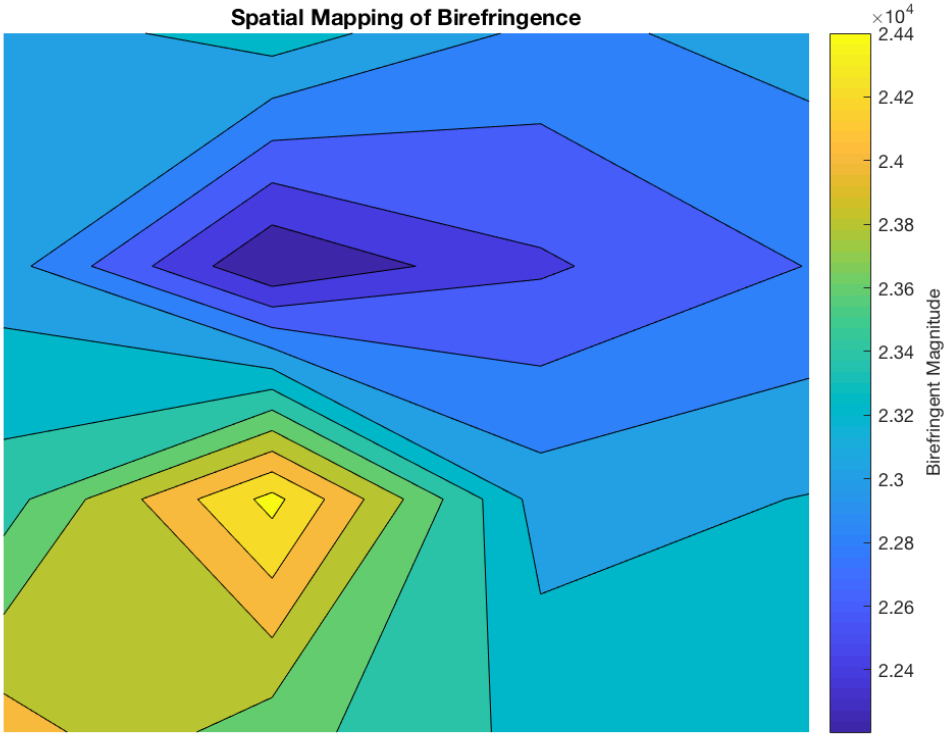

Figure 4.1.1 To the left is the first spatial mapping of the ThorLabs BB1-E03 dielectric mirror. The colorbar on the right display the magnitude of the birefringence in the form of a gradient. The brighter colors show a higher birefringence. The darker colors show a lower birefringence. It can be seen that the lower left portion of the mirror is more birefringent the upper right portion of the mirror.

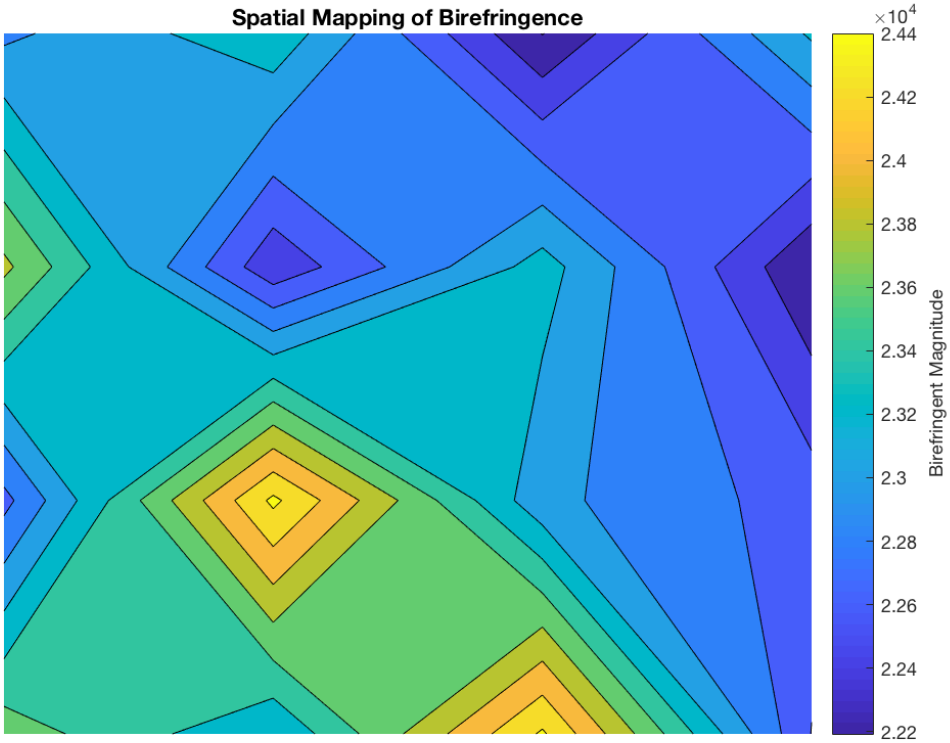

Figure 4.1.2 To the left is the second spatial mapping of the ThorLabs BB1-E03 dielectric mirror. The colorbar on the right display the magnitude of the birefringence in the form of a gradient. The brighter colors show a higher birefringence. The darker colors show a lower birefringence. It can be seen that the lower left portion of the mirror is more birefringent the upper right portion of the mirror.

mirror generated in MATLAB using the birefringent data collected by the heterodyne polarimeter. The PDI beat signal was about 600 mVpp and the PD2 beat signal was about 400 mVpp as read on the oscilloscope. Each point on the mirror was measured for two minutes. The mirror used for this spatial evaluation was a ThorLabs BB1-E03 dielectric mirror.

These contour maps are visual representation of how the birefringence changes across the surface of the mirror. The brighter colors reveal a higher birefringent area of the mirror while the darker colors show a lower birefringent area of the mirror. The birefringent values range from about 22,000 μrad to 24,000 μrad. There is a 7% fluctuation in birefringent amplitude across the area of the mirror we were probing.

The contour maps are two mappings over the surface of the same mirror. This was done to validate the consistency of our measurements. They reveal that this mirror has a lower birefringence in the middle to upper right portion, while a higher birefringence in the lower left portion. This indicates that the birefringence of the mirror is indeed spatially dependent upon where one desires to measure the birefringence of the mirror.

4.2 Magnetic Stress

It is necessary to note that for the magnetic stress measurements, we are no longer interested in how the birefringence changes at local points of the mirror, so we installed a telescope to increase the beam size to about 15mm. This will allow us to observe how the global birefringence changes due to the magnetic field. The mirror is also mounted in a different mount to maximize the surface exposure to the parallel magnetic field. The magnets were mounted far away from the mirror and then in 1/8" increments brought closer to the mirror. Each increment was measured for two minutes.

The PD1 beat signal was approximately 280 mVpp and the PD2 beat signal was about 230 mVpp. The decrease in signal is do to the enlarged beam size. The mirrors tested in the magnetic field were a New Focus 5104, a unmarked mirror made with fused silica, and a ThorLabs BB1-E03 dielectric mirror.

New Focus 5104

Figures 4.2.1-2 display plots of the New Focus 5104 mirror. *Figure 4.2.1* is a plot of the birefringence versus distance away from the mirror. The mean birefringence value is 18,200 μrad. The error bar in the y-direction is +/- 206 μrad. The error bar in the x-direction is +/- 1/16 in. *Figure 4.2.2* is a plot of the birefringence as a function of magnetic field. For the New Focus 5104 mirror the birefringent amplitude is seemingly unaffected by the induced magnetic field as extreme as 1kG.

Mirror of Fused Silica

Figures 4.2.3-4 display measurements with the unmarked mirror made with fused silica. *Figure 4.2.3* is a plot of the birefringence ver-

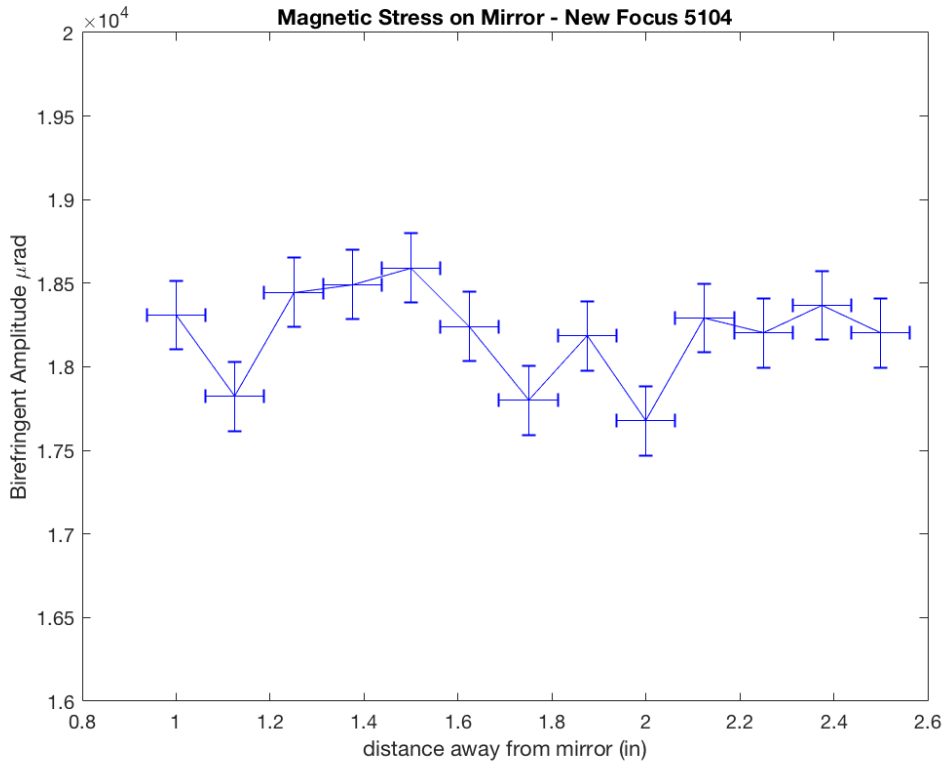

Figure 4.2.1 Above is a plot of the measurements taken for the New Focus 5104 mirror. The plot is birefringence versus the distance away from the mirror.

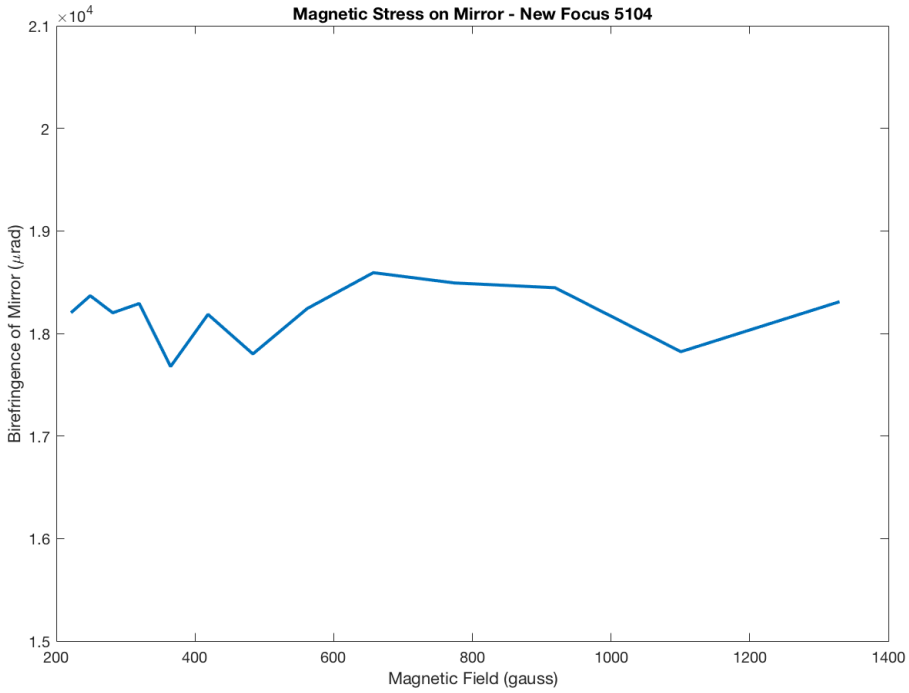

Figure 4.2.2 Above is a plot of the measurements taken for the New Focus 5104 mirror. The plot is birefringence as a function of the magnetic field.

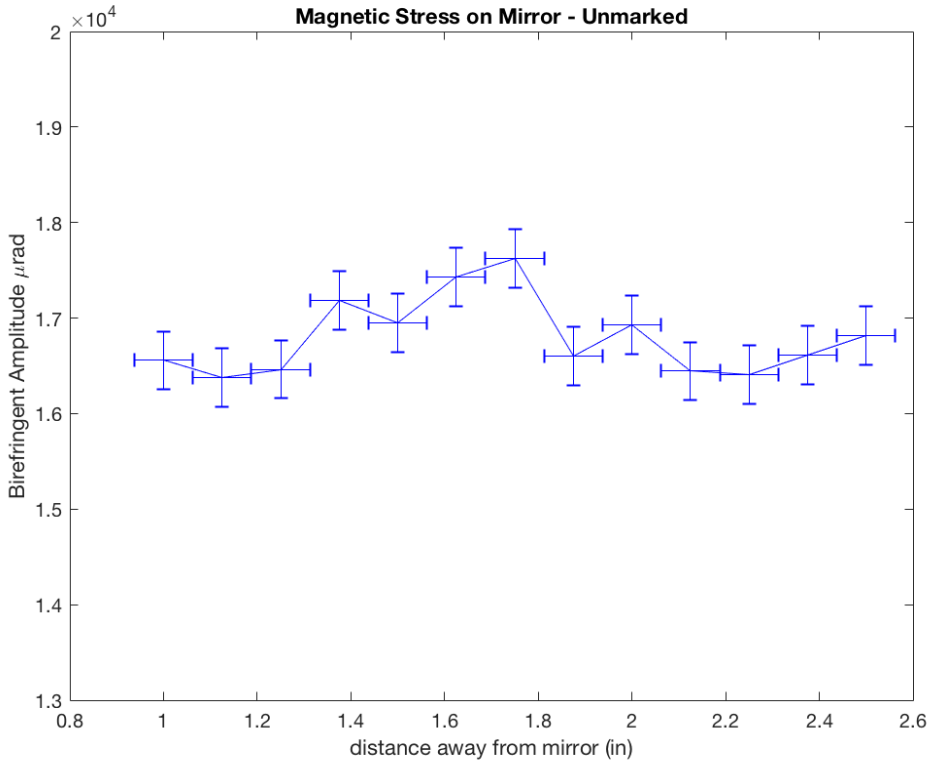

Figure 4.2.3 Above is a plot of the measurements taken for the unmarked mirror made with fused silica. The plot is birefringence versus the distance away from the mirror.

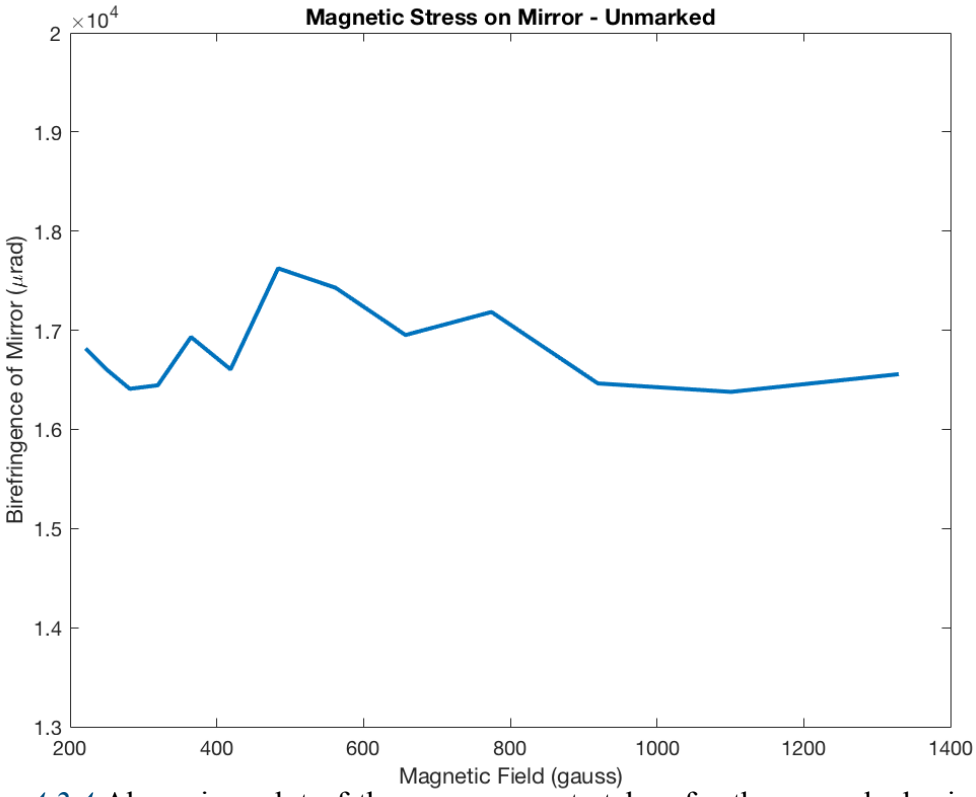

Figure 4.2.4 Above is a plot of the measurements taken for the unmarked mirror made with fused silica. The plot is birefringence as a function of the magnetic field.

sus distance away from the mirror. The mean birefringent amplitude is 16,500 μrad. The error bar in the y-direction is +/- 308 μrad. The error bar in the x-direction is +/- 1/16 in. *Figure 4.2.4* is a plot of the birefringence as a function of the magnetic field. The unmarked mirror made with fused silica remains unaffected with the induced magnetic field.

Thorlabs BB1-E03 Dielectric Mirror

The ThorLabs BB1-E03 was tested differently. The intrinsic birefringence of the mirror was found to be 16,650 μrad +/- 200 μrad. This was the average taken after 10 two minute runs. The mirror was then exposed to a magnetic field of approximately 1.25kG. The birefringence of the mirror was then measured while the mirror was exposed to the magnetic field. The birefringence of the mirror measured to be 16,500 μrad +/- 200 μrad. This was the average taken after 10 two minute runs.

The linear birefringence of the mirrors exposed to the magnetic field remain unaffected by the field. Therefore any affect the magnetic field could induce on the birefringence of mirrors is less than the intrinsic birefringence of the mirrors tested. It could be the case that as the global birefringence of the mirror decreases, the magnetic field effect will become increasingly more prominent. But within the sensitivity and precision of our experiment and the mirrors that were tested, the global intrinsic birefringence of the mirror remains the same. It could also be the case that the magnetic field induces a circular birefringent effect on the mirror coatings, which would remain undetected by our current experiment.

Conclusion and Outlook

Mirror birefringence, particularly spatial variations and exposure to magnetic fields, was characterized using a heterodyne polarimeter. For the ThorLabs BB1-E03 dielectric mirror, its intrinsic birefringence varies about 7% across the surface, meaning that the birefringence of the mirror is spatially dependent upon where the mirror is probed. When exposed to varying strengths of magnetic field the birefringence property of a New Focus 5104 mirror, a mirror constructed of fused silica, and the ThorLabs BB1-E03 remained unchanged.

To improve the sensitivity of the experiment, measurements will need to be taken for much longer and the noise floor of the Moku:Lab phase meter will need to be reduced. As the quality of the mirrors improves, the birefringent signal will become increasingly lower and it will be buried in the current noise floor. With much correspondence with Liquid Instruments Inc., they are improving the current Cascaded Integrator-Comb (CIC) Filter on the Moku:Lab. This will drastically reduce the noise floor, because it will filter out a lot of noise that becomes aliased down from higher frequencies.

These measurements lead us one step closer to measuring VMB for the ALPS experiment. As of now the magnetic field from the superconducting magnets poses no harm on increasing the linear birefringence of the mirrors. However, it will be necessary to measure the effects a magnetic field has on super-reflective mirrors much closer to the quality of the mirrors going to be used in the ALPS experiment. This will need to be done, because the magnetic field effect may currently be too subtle compared to the high birefringence of the mirrors we used and the current precision of our experiment. In addition, the experiment will have to be modified to measure circular birefringence, because the magnetic stress on the mirror may cause a circular birefringent effect, which can not be detected with our current experiment.

Potential improvements of this experiment may include, but are not limited to, reproducing the experiment in a clean room, rotating the mirror with a certain frequency similar to the rotating HWP, so that the intrinsic birefringence signal is separated from the magnetic stress induced birefringence or any other induced birefringent effect. It would be useful to track the absolute phase of the birefringence source, because with this information, how the angle of the birefringent vector is changing could be determined. The lab book for this project can be found at *https://darkcosmos.org/lab.*

Acknowledgments

I am forever grateful to Professor Selman Hershfield and the University of Florida department of physics for the priceless experience I have had as a 2017 Physics REU student. I can not thank Professor David Tanner and Professor Guido Mueller enough for allowing me to work on this ALPS project. An immense amount of thanks goes to my lab mates and now friends in ALPS, LIGO, and LISA, without them this work would not be possible. This work was funded by NSF grant DMR-1461019.

References

1 Murphy, D. B., Spring, K. R., Fellers, T. J., & Davidson, M. W. (n.d.). Introduction to Optical Birefringence. Principles of Birefringence. Retrieved July 25, 2017, from https://www.microscopyu.com/techniques/polarized-light/principles-of-birefringence.

2 Franck Bielsa, Arnaud Dupays, Mathilde Fouch´e, Remy Battesti, C´ecile Robilliard, et al.. Birefringence of interferential mirrors at normal incidence Experimental and computational study. Applied Physics B - Laser and Optics, Springer Verlag, 2009, 97 (2), pp.457-463.

3 Baum, C. (2016). Intrinsic mirror birefringence measurements for the Any Light Particle Search (ALPS). Retrieved May 28, 2017.

4 http://www.liquidinstruments.com

5 https://alps.desy.de

6 https://www.olympus-lifescience.com/fr/microscope-resource/primer/lightandcolor/mirrorsintro/